

Impact of Lump Characteristics on Self-Shielding Corrections of Active Neutron Interrogation on Fissile Material in Waste – 15405

Daniel Murphy *, Ludovic Bourva **, Stephen Croft ***

* School of Physics and Astronomy, University of Birmingham, Edgbaston, Birmingham B15 2TT, United Kingdom

** Canberra UK Ltd - AREVA Group, Harwell Oxford, Building 528.10 unit 1, OX11 0DF United Kingdom

*** Oak Ridge National Laboratory, Oak Ridge, TN 37831, United States of America

ABSTRACT

Non-destructive active neutron assay techniques such as active neutron coincidence counting, differential die away analysis or the californium shuffler method rely on the interrogation of fissile nuclear materials by an external neutron source. Whether it is a spontaneous fission or (α ,n) neutron source, like ^{252}Cf or AmLi; or a fusion neutron generator, all of these techniques rely on induced secondary fission events to provide prompt or delayed neutron signals that serve as the basis for the fissile material quantification. The accuracy of these fissile mass measurements is therefore dependent on the neutron interrogation efficiencies determined for calibration reference standards and whether the measured items are comparable to the calibration condition. In such favorable conditions, it is possible to establish a reliable empirical non-linear relationship between apparent (uncorrected) and real or true fissile mass. However, in waste measurements, this is unlikely to be the case; thus a calibration approach that takes account of the neutron self-shielding effect is required. By incorporating the Self-Shielding Factor (SSF) of the calibration reference standards, a linear mass calibration factor [$\text{s}^{-1} \cdot ^{239}\text{Pu}_{\text{eq}} \text{g}^{-1}$] can be found; this calibration is accurate for waste in which the fissile material is “infinitely dilute” i.e. the waste exhibits no self-shielding; this is assumed to be representative of dispersed material. The self-shielding correction and its systematic uncertainty are then left to be treated as part of the Total Measurement Uncertainty (TMU) evaluation associated with the assay result.

The derivation of the TMU contribution associated with the self-shielding effect in nuclear waste is a complex problem for which a reliable evaluation has to be performed. This is usually based on assuming “worst case scenarios” for the distribution of material that can arise in a particular waste stream. Such an approach is conservative, but often very penalizing, especially if one considers larger lumps (those containing grams of fissile material); for such lumps, the self-shielding correction becomes very significant, potentially altering the mass of $^{239}\text{Pu}_{\text{eq}}$ by over an order of magnitude. A worst case ‘nuclear safety value’ may not be the most appropriate choice for building a consignment best estimate or repository sentencing value for an item.

In the present work the authors describe a numerical approach to study the variability of neutron self-shielding factors associated with distributions of a wide range of lump characteristics in terms of size, shape, chemical composition, density and isotopic composition. The described novel calculation tool is capable of accurately predicting the real impact of random distribution of lumps in a waste material, and allowed to show that given reasonable, defensible, assumptions on the composition of the lumps in waste stream, the systematic error component of the DDA TMU can be significantly reduced.

INTRODUCTION

Active neutron interrogation techniques all rely on sampling the measured item by inducing fission in any fissile isotope present and detecting secondary neutrons (prompt or delayed) produced by these fission events. The number of neutrons produced by a sample in a given interrogating neutron flux therefore depends on which nuclides are present, and in what quantity. Consequently, the results of such assays are commonly expressed in terms of ^{235}U equivalent mass or ^{239}Pu equivalent mass, as defined below:

$$^{239}\text{Pu}_{\text{eq}} = \sum_i m_i \frac{\sigma_{fi} \bar{\nu}_i A_{239\text{Pu}}}{\sigma_{f239\text{Pu}} \bar{\nu}_{239\text{Pu}} A_i} \quad (\text{Eq.1})$$

where m_i , σ_{fi} , $\bar{\nu}_i$ and $A_{239\text{Pu}}$ are the mass, microscopic fission cross section, average number of neutrons produces per fission, and the atomic mass of the i^{th} fissile nuclide respectively. With this definition, 1 g of infinitely dilute $^{239}\text{Pu}_{\text{eq}}$ produces fission neutrons at the same rate as 1 g of infinitely dilute ^{239}Pu for a given interrogating neutron flux.

In a Differential Die Away (DDA) counter [1, 2, 3], fast neutrons are injected into the assay chamber using a pulsed source, such as a deuterium-tritium (D-T) fusion generator producing 14 MeV neutrons. These neutrons are quickly moderated to thermal energies within the chamber so that they can efficiently induce fissions in any fissile material present in the sample, which for waste assay is typically a 55-gal/208-l drum filled with a waste matrix. The short pulse of interrogating neutrons is quickly moderated within the assay chamber, building up a thermal flux with a much longer die-away time constant than the interrogation neutrons. The DDA assay technique hence relies on segregating fast neutron detection events associated with the interrogation source (interrogation background) with later fast neutron detection events associated with thermal neutron induced fissions (fissile signal). This is illustrated in Figure 1.

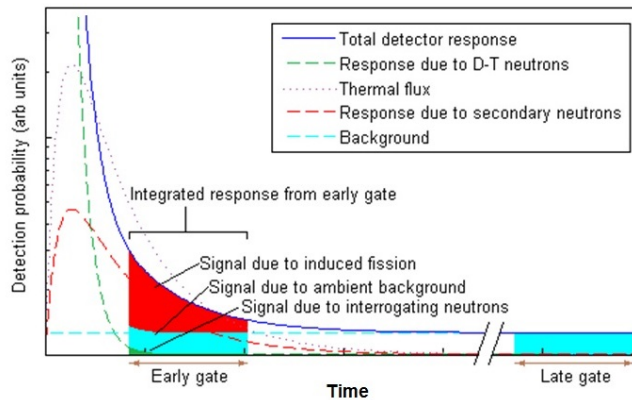


Figure 1. Detection time profile in FNDP illustrating the DDA technique signal interpretation

Practically, fast neutron detection is usually performed by Fast Neutron Detection Packages (FNDPs), which consist of a thermal neutron detector or a cluster of such, such as a ^3He tube, surrounded by moderating High Density PolyEthylene (HDPE) and tightly clad in a cadmium wrapper. Their associated counting electronics is set up to perform time acquisition with two main counting gates. An “early gate” is used to record the fissile signal. Depending on the chamber design, it is positioned between 500 and 1200 μs relative to the generator pulse trigger time, so as to minimize counts from the pulsed neutron source and maximize counts from induced fissions. At a later time, of the order of a few milliseconds, a late gate is opened to measure the ambient neutron background, for example, from spontaneous fission sources in the waste drum. The ambient background rate is subtracted from the count rate in the early gate to give

the count rate due to induced fissions. Using this approach a fissile mass calibration can be derived by relating the measured intensity of the background corrected early gate fissile signal with the $^{239}\text{Pu}_{\text{eq}}$ of measured reference standards. However the linearity of such a relationship only holds if the neutron interrogation of the fissile material remains uniform. Indeed, the induced fission neutron production rate is linearly proportional to the mass of $^{239}\text{Pu}_{\text{eq}}$ only if the fissile material itself has no influence on the neutron interrogation. Any realistic case will present material with finite size lumps for which the outer surfaces of the lumps will attenuates the interrogating neutron flux through fission and capture events, thus partially shielding their deeper portion. The probing flux is therefore expected to show an exponential behavior with attenuation coefficient λ shown below:

$$\lambda = 1/(\Sigma_f + \Sigma_c) \quad (\text{Eq.2})$$

where Σ_f and Σ_c are the effective fission and capture macroscopic cross sections respectively. As a result, the whole mass of a lump cannot be probed uniformly by the flux and the rate of fission will be reduced when compared to a theoretical infinitely dilute case. This effect is quantified by the Self-Shielding Factor (SSF):

$$SSF = \frac{R_{\text{lump}}}{R_{\text{dilute}}} \quad (\text{Eq.3})$$

Where R_{lump} is the rate of neutron production by induced fission in the particular lump under consideration when exposed to a particular neutron interrogating flux and R_{dilute} is the rate of neutron production that would occur if the material constituting the lump were infinitely dilute. Note that the value depends on the mass, the geometry, the chemical form, and the density of the lump, as well as, the spectrum of the neutron interrogating flux.

SSF calculation by numerical methods has been used to evaluate the impact of this effect in nuclear material aggregates [4, 5]. As illustrated in Figure 2, corrections for this effect have been shown to become very large when dealing with gram sized and dense aggregates.

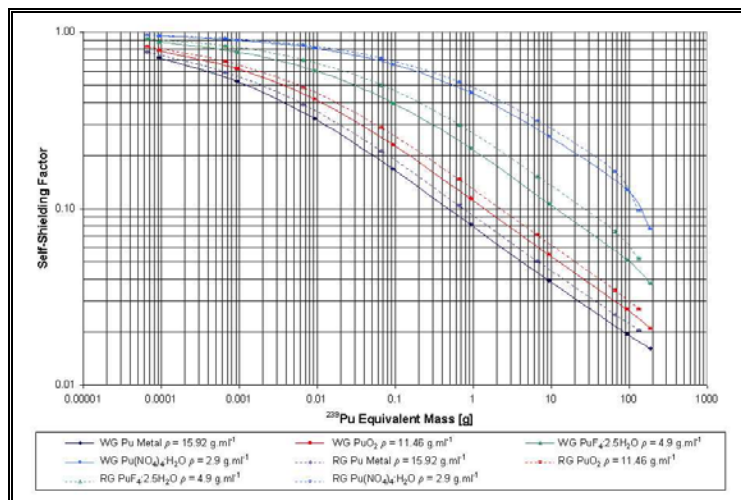


Figure 2. Self-shielding factors for spherical aggregates of various types of plutonium bearing material and masses [3]

Also note that accurate SSF calculations also play a key role in deriving reliable “dilute” mass calibration factors when correcting reference sample measurements, as these standards usually exhibit significant self-shielding.

With regards to the TMU associated with DDA assay results, the systematic uncertainty component of the

TMU associated with self-shielding is often derived based on assuming a worst case scenario. This corresponds to assuming that the entire apparent mass derived from the dilute mass calibration is being co-located into a single dense spherical lump. A deviation of such a magnitude is somewhat assumed to correspond to a $\pm 3\sigma$ level of variation, so that the relative systematic uncertainty due to self-shielding, σ_{SSF} , is given by:

$$\sigma_{SSF} = \frac{CF_{SSF}(worst)-1}{3} \quad (Eq.4)$$

The assumption that the mentioned “worst case” scenario represents a $\pm 3\sigma$ variation is somewhat arbitrary, and implies that the σ_{SSF} is Gaussian by nature. Nevertheless, the approach is conservative, and for most cases highly penalizing, as shown in Figure 3.

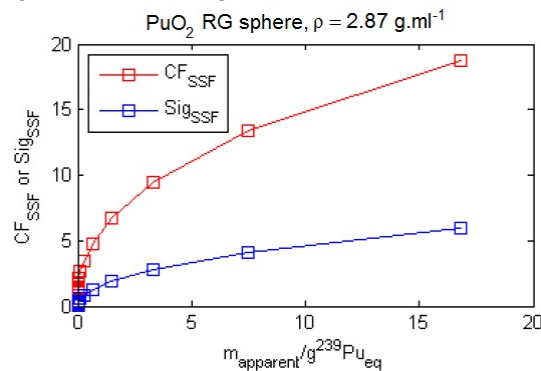


Figure 3. The worst case scenario for different apparent masses of ²³⁹Pu_{eq} and the σ_{SSF} derived from it

In view of such a penalty, the authors have considered how to develop a SSF evaluation scheme based on Monte Carlo Calculations under which the σ_{SSF} derivation could be performed based on defensible assumptions about the distribution of lump characteristics present in a particular waste stream.

SELF SHIELDING CALCULATIONS

Methodology

Self-shielding factors can be calculated using Monte Carlo methods applied to radiation transport. In this work the MCNPX v2.7.0 code [6] was used to simulate the interrogation of fissile lumps. In the computational models, a simple geometry consisting of a single lump of fissile material surrounded by an isotropic surface source has been defined, as illustrated in Figure 4.

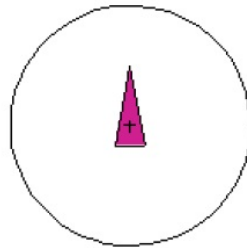


Figure 4. Illustration of MCNPX geometries for a conical lump and a spherical source surface with M=2

In this example, the black sphere represents the spherical neutron source. It is centered on the mass centroid of the cone and its radius is twice the value that would result in it grazing the surface of the lump.

The lump is hence bathed an isotropic flux of neutrons and a type 4 neutron track length tally is used to score the neutrons per unit volume of the lump. The tally is weighted according the energy dependent total fission microscopic cross section, $\sigma_f(E)$; and the average number of neutrons produced per fission, $\bar{\nu}(E)$; both of these quantities are averaged for every atom present in the lump. Thus, the tally evaluates the number of prompt fission neutrons produced per source neutron introduced per target atom in the lump. This can be written as:

$$T_{Lump} = \frac{\int_{E=0}^{E=\infty} L(E) \cdot \sigma_f(E) \cdot \bar{\nu}(E) \cdot dE}{V \cdot NPS} \quad (\text{Eq.5})$$

where $L(E)$ is the neutron track length per unit energy, NPS is the number of source neutrons used in the simulation, V is the lump's volume. The result of this tally is, of course, subject to self-shielding. In order to evaluate the SSF, a similar simulation is run with a vacuum in place of the lump volume. The weighting of the tally is the same, so the only difference is that the flux is not perturbed by the presence of the lump. This corresponds to the case of an infinitely dilute material; the tally result is referred to as T_{vacuum} . The ratio of the two tallies is the self-shielding factor.

Note that the proposed methodology introduces the dependency of the SSF value to $\bar{\nu}(E)$ variation as the interrogation neutron energy is perturbed by the lump. This dependence was not considered in earlier work [Bourva] and resulted in small variation in SSF as shown in Figure 5.

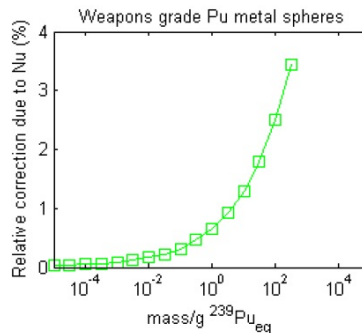


Figure 5. Relative correction introduced in SSF evaluations by factoring $\bar{\nu}(E)$ dependence for dense lumps of low burn-up plutonium

Note that the impact of this modification was only significant (up to a few percent corrections) when dealing with large (> 1g) and dense lumps of fissile material.

Additionally, in order to generate an isotropic flux at the lump position in the MCNPX models the size of the neutron source surface relative to the dimension of the lump has to be large enough to not introduce significant geometrical bias. Optimally the source surface should be a very large sphere with a radius significantly larger than the lump size itself. However, the larger is the source surface the smaller is the probability of interaction with the lump, thus making the computation largely inefficient. We therefore investigated the possibility to define an optimum source size definition by modeling the evolution of the computed SSF, and its associated statistical uncertainty, as a function of the source dimension. The source dimension was scaled to the size of the lump by introducing a scaling factor M . The M value is defined as unity for a source radius for which the source sphere is grazing any surface point of the lump. Figure 6 shows the evolution of the SSF results for two lump sizes with variable values of M between 1 and 100.

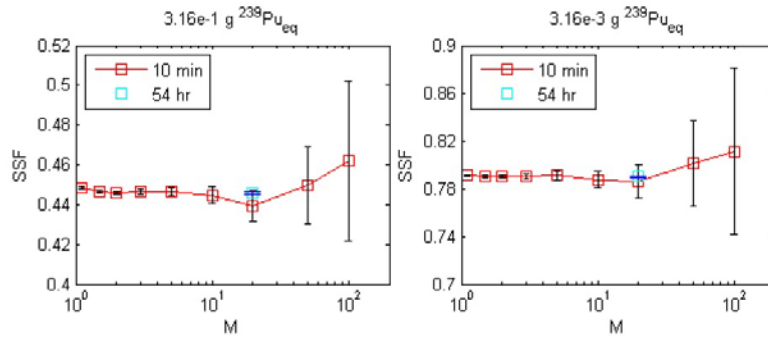


Figure 6. Variation of the computed SSF for two conical lump sizes as a function of the relative source radius

The initial set of calculation where performed using 10 minutes of computation and repeated at $M=20$ for 54 hours to confirm the statistical stability of the SSF results. From this investigation it was concluded that models with M equal to 2 should yield geometrically unbiased results, while delivering the most efficient computations.

It is noteworthy that the sphere is likely to exhibit the greatest dependence on M , as this geometry has the largest percentage of its volume in proximity to the source surface.

Lump Characteristics

To study the dependence of SSF to specific lump distribution hypotheses, the calculation approach described above was applied to generate reference data for a broad range of lump characteristics. These characteristics included the chemical form, isotopic composition of the nuclear material and the shape, mass and density of the lump. The energy spectrum of interrogating neutrons was also considered. The following tables summarize the range of parameters used during this work.

Table 1. Physical/Chemical characteristics of the lumps under investigation in this study


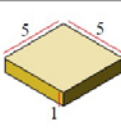
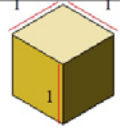
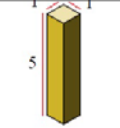
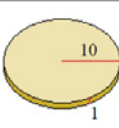
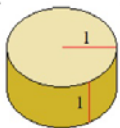
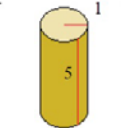
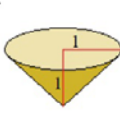
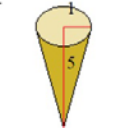
Chemical form	Formula	Ref Density (g cm^{-3})	Isotopics
Plutonium Metal	Pu	15.92	RG, RGold, WG
Plutonium Dioxide	PuO_2	11.46	RG, RGold, WG
Plutonium Fluoride	$\text{PuF}_4 \cdot 2.5\text{H}_2\text{O}$	4.9	RG, RGold, WG
Plutonium Nitrate	$\text{Pu}(\text{NO}_3)_4 \cdot \text{H}_2\text{O}$	2.9	RG, RGold, WG
Uranium Metal	U	19.05	DU, HEU
Uranium Dioxide	UO_2	10.96	DU, HEU
Uranium Trioxide	UO_3	8.7	DU, HEU
Uranyl Oxide	$(\text{UO}_2)_3\text{O}_2$	8.38	DU, HEU
Uranium Tetrafluoride	UF_4	6.7	DU, HEU

Table 2. Isotopic compositions of the nuclear material in the simulated lumps

Plutonium Materials			Uranium Materials			
Nuclide	Weight Percentage			Nuclide	Weight Percentage	
	WG	RG	RGold		DU	HEU
²³⁸ Pu	0.013	2.42	2.4224	²³⁴ U	0.0055	0.0003
²³⁹ Pu	93.734	50.03	50.0890	²³⁵ U	0.3000	93.5742
²⁴⁰ Pu	5.996	27.33	27.3623	²³⁶ U	0.0018	0.0035
²⁴¹ Pu	0.224	11.99	1.3409	²³⁸ U	99.6927	6.4220
²⁴² Pu	0.033	8.23	8.2396			
²⁴¹ Am	0.000	0.00	10.5457			

Every chemical form was simulated at reference density, indicated in Table 1, 0.75 times, 0.5 times and 0.25 times the reference density. These lower densities represent different physical forms for the material. For example, PuO₂ could occur as a green or loose powder (low density) or as a fragment of a sintered pellet (high density). A number of small particles could also bond loosely together such that their behavior is similar to a larger lump of the same material with a density lower than its usual bulk density. A series of nine geometries were also considered in this study. Table 3 shows a graphical representation of these geometries with the assumptions on their aspect ratio.

Table 3. Isotopic compositions of the nuclear material in the simulated lumps

Sphere	Square Plate	Cube	Long Cuboid	Circular Disc
				
Squat Cylinder	Long Cylinder	Squat Cone	Long Cone	
				

For each configuration, the effect of lump mass (in ²³⁹Pu_{eq}) was examined over the range 1x10⁻⁵ g to 316 g. MCNPX simulations were run for masses between these values in half-decade steps i.e. 1x10⁻⁵ g, 3.16x10⁻⁵ g, 1x10⁻⁴ g, 3.16x10⁻⁴ g and so forth, making a total of 16 different masses.

Altogether 22 materials, 9 geometries, 4 densities, 16 masses, and 2 simulations runs for every SSF data point resulted in 25,344 MCNPX runs being generated. The results of these represent the main database entries. Each computation was run for 10 minutes to obtain reliable statistics (relative uncertainty ≈ 0.1% on SSF), for a total of 176 days of computer time. Several multicore computers were used to accelerate the process over a 4 week period.

In the case of waste assay, the interrogation neutrons energy distribution can be seen as an additional input parameter on SSF calculation as matrix material will not only perturb mass calibration assumptions (i.e. matrix corrections) but also systematic error due to self-shielding variation. Variability of SSF with matrix material/ interrogation neutrons energy distribution was investigated by deriving SSF for a given lump when assuming variable energy spectra tallied in 7 different waste matrices (combustibles/concrete/hdpe/heavy metal/light metal/mixed metals and PVC). This indicated, as shown in

Figure 7, that the SSF values for a given lump is potentially affected by the waste matrix, with absolute effects being most notable for large and dense lumps.

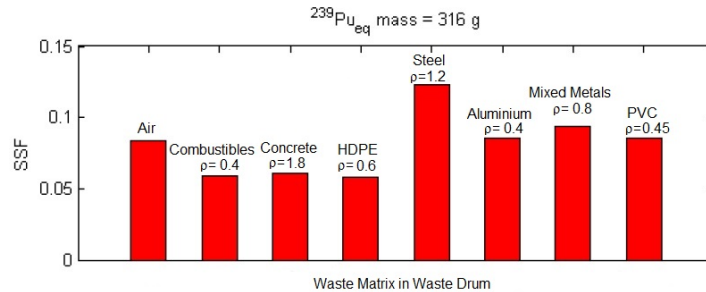


Figure 7. Variation of the SSF for averaged neutron interrogation energy spectra associated with 7 different materials and air for a spherical lump of reactor grade (old) PuO₂ powder, density 2.87 gcm⁻³, ²³⁹Pu_{eq} mass 316 g

Ideally, a whole database should be built accounting for every spectrum, but this was not possible due to computing time constraints. Therefore, despite acknowledging this additional degree of freedom in the calculation, a single averaged HDPE spectrum was selected as the representative interrogation neutron energy distribution used for the remainder of this work. Also note that, as the least penetrating case, it is the most vulnerable to self-shielding and therefore should provide a conservative estimate on CF_{SSF}.

SSF Database Results

To facilitate the quantitative treatment of the data, it has been judged convenient to introduce numerical quantities that provided a metric for lumps shapes and key material characteristics. The first of this new parameter is the shape index, I_S. The effect of the lump's shape on the SSF is expected to be related to the ratio between the surface area and the volume of the lump. For each shape, this ratio has been calculated and normalized to the spherical lump case to define the shape index of the lumps. The shapes considered in this work have I_S values of between 1.00 for the sphere and 3.09 for the disc.

The material and density of each lump can both be by using the ²³⁹Pu_{eq} density of the lumps. The following relationship was used to derive it

$$\rho_{239\text{Pueq}} = \rho_0 \sum_i F_i \frac{A_{239\text{Pu}} \sigma_i \bar{v}_i}{A_i \sigma_{239\text{Pu}} \bar{v}_{239\text{Pu}}} \quad (\text{Eq.6})$$

Where the i index runs over all nuclides present in the lump, ρ₀ is the ordinary density of the material, F_i is the weight fraction of nuclide and all other symbols have the meanings previously associated with them. ρ_{239Pueq} will, henceforth, be referred to simply as ρ, for convenience.

Using these two parameters and the ²³⁹Pu_{eq} mass of the lumps, allowed to parameterize and plot the all 12672 SSF data points derived in the course of this study to produce a main SSF database. A three dimensional representation of these results is shown in Figure 8.

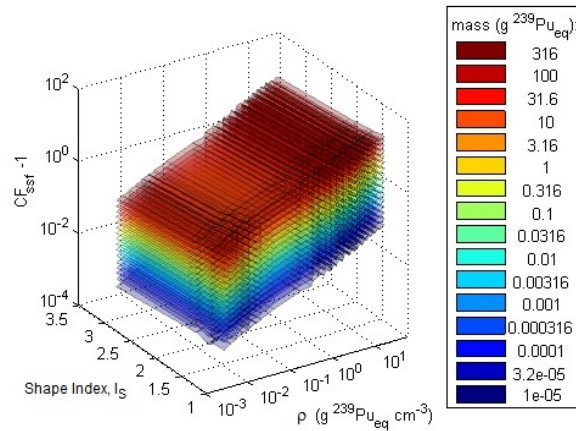


Figure 8. Visualization of the main database of SSF results

When plotted using logarithmic scales for ρ and $(1/SSF)-1$ and a linear scale for I_s , the surfaces of constant mass (indicated by different colors in Figure 8) form approximately parallel planes. Logarithmic mass increments give equal spacing between the planes. This suggested a functional form that can be used to fit the entire data set, as proposed in Equation 7.

$$SSF = \frac{1}{1 + q_1 \rho^{q_2} m^{q_3} q_4 I_s} \quad (\text{Eq.7})$$

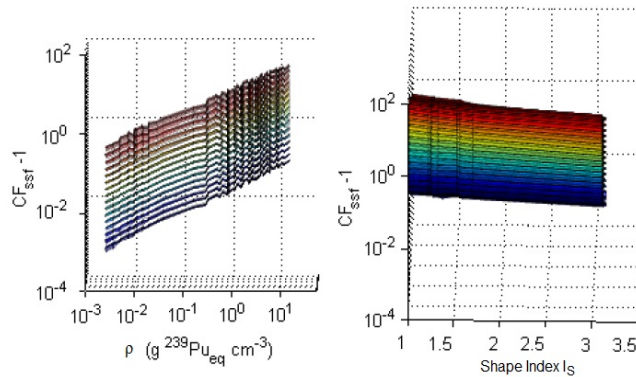


Figure 9. Side views SSF database results showing their variation with respect to ρ and I_s

The left hand plot of Figure 9 shows that there is some degree of “crinkling” in the computed SSF mass planes. This is due to the fact that all of the information about the different materials and densities has been rolled together into just one plotting parameter. This effectively assumes that the non-fissile materials in the lumps do nothing little other than padding out the fissile material in space. This is not true, as these materials still capture, scatter and moderate neutrons. In contrast, the right hand plot of Figure 9 shows that the variation with respect to its shape index quite linear. Using this extended data set a least square fitting algorithm returned the following values for the q_i parameters of Equation 7.

$$\begin{bmatrix} q_1 \\ q_2 \\ q_3 \\ q_4 \end{bmatrix} = \begin{bmatrix} 2.9378 \\ 0.5636 \\ 0.3320 \\ 0.6203 \end{bmatrix} \quad (\text{Eq.8})$$

The quality of the proposed fit was evaluated by estimating the relative difference obtained between SSF

values obtained using the q_i parameters and Equation 7 against MCNPX values. The obtained distribution is plotted in Figure 10.

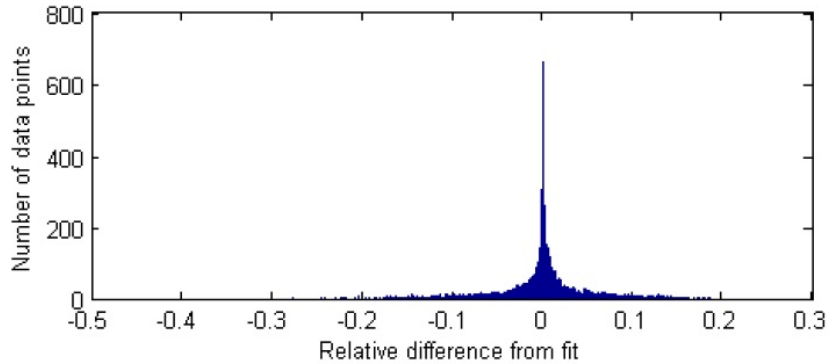


Figure 10. Distribution of relative differences between SSF values derived using MCNPX and SSF values derived from the functional fit of the SSF database.

From Figure 10 it appears that the distribution is neither symmetric nor Gaussian. However, it has been estimated that the proposed fit provides SSF values within 15% of the MCNPX values for 95% of the considered cases. The advantage of this approach is that it can be used to determine approximate SSF of lumps made of any material, geometry and density.

LUMP DISTRIBUTION SIMULATIONS

SSF Database Interpolation

While the simplicity and flexibility of the functional fitting approach discussed above certainly has its merits, greater accuracy than $\pm 15\%$ was considered a requirement for this work. In order to accomplish this, a numerical interpolation routine was developed. A C program was written to perform the interpolation on the MCNPX simulation data that was initially stored as an ASCII file. When asked to compute the SSF for an arbitrary target lump, the program queries the data file for any MCNPX results associated with a lump that match the target lump on every parameter other than its mass. This data set that is extracted is similar to one of the plot shown in Figure 2. A simple nearest neighbor interpolation algorithm is applied, as represented in Equation 9.

$$SSF_{interp}(m) = SSF_b + \frac{SSF_a - SSF_b}{\log(m_a) - \log(m_b)} \times (\log(m) - \log(m_b)) \quad (\text{Eq.9})$$

In this expression, m is the $^{239}\text{Pu}_{\text{eq}}$ mass of the target lump and m_a and m_b are the $^{239}\text{Pu}_{\text{eq}}$ masses nearest to m that were extracted from the database; m_a is above m and m_b is below m . SSF_a and SSF_b are the self-shielding factors calculated for these neighboring lumps. This interpolation method results in straight lines between assumed between points on a semi-log plot such as the one shown in Figure 2. The interpolation method presented above can evaluate the SSF of many arbitrary lumps very quickly and is as accurate as the underlying data set.

Complex Lump Distribution Simulations

Using the SSF database interpolation method, it has been possible to evaluate SSF for individual lumps, or to study how variation in shape or chemical composition of single lumps impact the SSF. However the real benefit of exploiting the range of computation performed during this work has been in developing a

new application that allows through random sampling the combining of a versatile definition of lump distributions with the SSF interpolation method to provide statistical distribution of SSF. The result is to provide a tool that allows studying how more or less complex distributions of lumps characteristics within a waste drum may impact the overall DDA assay accuracy by providing evaluation of systematic self-shielding uncertainties associated with such lump distributions. We also expect that real distribution of lumps in waste can be reasonably characterized as the results of operational knowledge, physic-chemical models, sampling analysis or combinations thereof to provide defensible input parameters.

The numerical application relies on a user supplied ASCII text file that provides the basis for describing complex lump distributions. The ASCII file is read by the C program and a branching data structure linked by pointers is created. An example of such a lump distribution specification is shown graphically in Figure 11. The format is very flexible and allows for simultaneous modelling of different shapes, chemical forms, densities, and mass histograms, which are specified in the same way as a source energy histogram of an MCNPX input file.

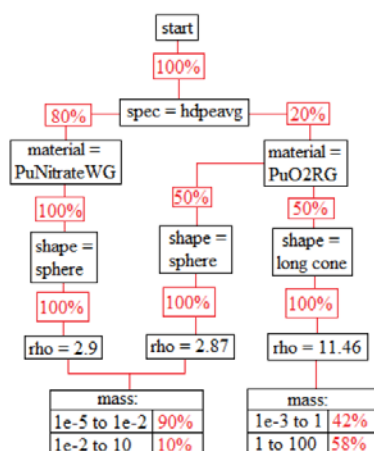


Figure 11. Graphical example of the branching data structure used to specify the characteristics of lump distributions.

When generating a lump from the specified distribution, the program moves through the branching structure much like a flow chart, assigning one property of the lump at each node and then rolling a random number to decide which path to proceed on. When it reaches the point of assigning the lump's mass, it first rolls one random number to choose which bin of the histogram to put the mass in and then rolls a second random number to give a uniformly distributed mass between the bin boundaries.

When running the program with a particular lump distribution file, the user also specifies a target fissile mass in the drum, which can be defined either as true mass or apparent mass of $^{239}\text{Pu}_{\text{eq}}$. The program then proceeds to randomly generate lumps according to the distribution and add them to the hypothetical waste drum. When the drum is "filled" to the desired content of fissile material, the real and apparent masses are recorded. This process is repeated for N drums or for T seconds to generate a distribution of SSF for those lumps distribution assumptions.

When finished, the mean drum SSF and its standard deviation are reported to the user; the drum SSF is defined as the ratio of apparent fissile mass in the drum to true fissile mass in the drum. More detailed output can also be provided, including the full distribution of real and apparent drum masses.

In order to illustrate the capability of the software in investigating the effect of different lumps distributions, four representative mass histograms were chosen: a flat distribution, with equal likelihood for any element of mass, dm , to be found in a lump of any mass between defined lower and upper limits; an upwards sloping distribution, with greater probability for higher mass lumps; a downward sloping distribution, with greater probability for lower mass lumps; and a delta function, where all lumps have the same mass. These four distributions are shown in Figure 12.

The examples shown in Figure 12 all have an upper limit on lump mass set to 1 g. The sloping distributions are always constructed such that the value of $m(dn/dm)$ changes by a factor of 10 between the lower and upper limits.

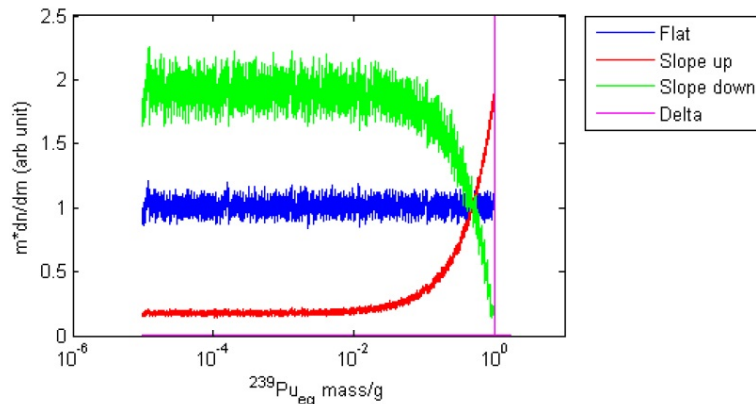


Figure 12. Graphical representation of four “reference” lump mass distributions for lumps with a 1 gram upper mass limit

For illustrative purposes only, we considered the case of aged reactor grade PuO_2 lumps with a spherical geometry and a physical density of $2.87 \text{ g}\cdot\text{cm}^{-3}$. This is likely to be a common powder material, and the choice of the spherical geometry ensured a conservative estimate of the self-shielding. This hypothetical case is used in the coming sections as a reference assumption to study the impact of some of the other parameter used to describe the lump distribution characteristics and their impact on SSF evaluations.

The way in which a population of lumps in a drum is constructed is stochastic in nature. It is, therefore, expected that the results will exhibit statistical fluctuation. In almost all cases that were considered, it was found that the variation of the SSF calculated for a given waste drum was Gaussian. The distribution of SSF values diverged from this form only when the upper limit of mass was comparable to or exceeded the total mass in the drum. Indeed when the maximum lump mass is allowed to approach or exceed the total fissile mass present in the drum, a significant number of drums emerge with only a very small number of lumps in them. Thus, divergence from Gaussian statistics is not surprising. This is illustrated in Figure 13 where SSF distributions assuming flat mass distribution but with different lump upper mass limits are shown.

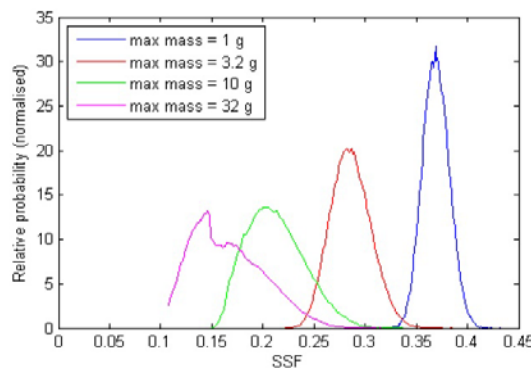


Figure 13. Statistical variation of SSF evaluated for 10^5 waste drum containing 10 g of $^{239}\text{Pu}_{\text{eq}}$ in the form of PuO_2 spherical lumps with a density of $2.87 \text{ g}\cdot\text{cm}^{-3}$ and different limits on the lump maximal size.

When these pathological cases are avoided, it is observed that, as the distribution is indeed Gaussian, it

can be fully described by reporting just its mean $\langle \text{SSF} \rangle$ and standard deviation σ

SSF SYSTEMATIC ERROR

As was discussed earlier, self-shielding effects are not directly accounted for in correcting DDA assay results but are typically handled as part of the total measurement uncertainty calculation for a measurement. Thus, σ_{SSF} , the relative systematic uncertainty due to self-shielding, is attributed to an assay result on the basis of comparison of calibration assumptions (dilute material) to potential departure from this calibration assumption, for which the single lump assumption is taken as a worst case scenario.

In the present approach the observed SSF distribution ($\langle \text{SSF} \rangle, \sigma$) provide for a given set of assumption on the lump distribution a reliable statistical tools to evaluate σ_{SSF} .

Clearly in real measurement cases the lack of knowledge about the specific lump distribution present in a given waste drum is the limiting factor in providing accurate SSF values and CF_{SSF} correction factors. However, in some circumstances, it may be possible to define an upper bound on the mass of lumps that can occur in a waste stream. For example, if the waste is sieved as part of its processing, then one can have a good degree of confidence in assuming that no lump larger than a specific size can be present in the waste stream. To illustrate this, we modelled our reference lumps case assuming an apparent mass result of $10 \text{ g } ^{239}\text{Pu}_{\text{eq}}$. The σ_{SSF} value associated with such an assay for this type of material would be a factor 4.5. Assuming any of the 4 aforementioned lump distributions and a variable maximum lump mass/size was shown to significantly reduce this value, as shown in Figure 14.

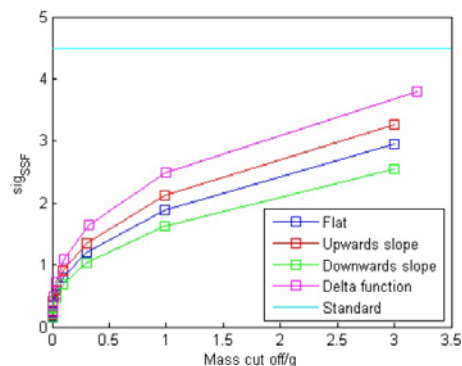


Figure 14. Impact of lump mass upper limit on the systematic error associated self-shielding effect.

These results also show that even without knowing the exact lump size distribution in a drum the limiting assumption that lumps cannot be above a certain size do significantly improve the TMU. To further illustrate this point, calculations to tally the evolution of σ_{SSF} with the mass of fissile material in a drum have been performed. Figure 15 shows how σ_{SSF} remains capped based on a maximum lump size/mass criterion even in the case of waste drum with large quantity of fissile material. These calculations were performed on the basis of a flat lump mass distribution and our reference lump material.

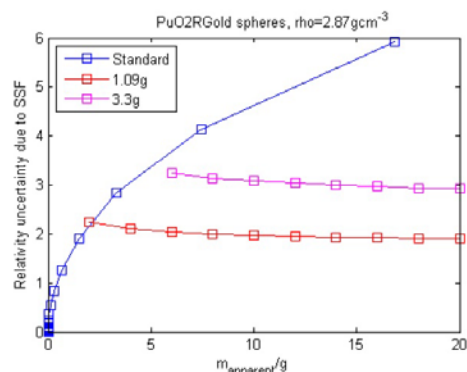


Figure 15. Comparison of the behavior of σ_{SSF} as derived using a single lump assumption and the proposed stochastic method for drums with different apparent masses of $^{239}\text{Pu}_q$ and a lump upper mass limit

CONCLUSION & FUTURE WORK

The analytical approaches usually employed to report systematic uncertainties associated with self-shielding for DDA assays use the rather arbitrary assumptions that the potential lumps present in the a waste drum are comparable in chemical form and density to the reference standards that were used to establish worst case scenarios. Additionally, these worst case scenarios are based on a single lump assumption which is arbitrarily associated with a 3σ statistical variation in SSF. Neither of these assumptions is truly based on evidence and seems to be applied more because of convenience and because of the absence of any viable alternative.

The software tools presented here make it possible for the first time to calculate the SSF for arbitrary lumps distributions for a wide range of chemical and physical characteristics of lumps of plutonium and uranium bearing materials. This makes possible a more sophisticated stochastic approach in determining self-shielding effect in real waste. Such an approach, when combined with reasonable arguments limiting the size attributed to any single lumps in a waste stream, was also shown to significantly lower the upper bounds placed on the systematic self-shielding corrections to be made on assay results. This may significantly improve reported TMU, especially for uncorrected assays returning apparent fissile masses well above gram quantities. The implications are better

Among the area of improvement to the current numerical analysis it was noted that the current interpolation algorithm used in this work only interpolates with respect to a single lump parameter, namely the lump mass. Thus, it is necessary to have a large pre-computed database containing exact matches for all other parameters (chemical form, density, shapes...). It would be very advantageous to develop the software further to provide interpolation capabilities between chemical forms, densities, shapes...

Additionally, the main database records were derived for a single distribution of interrogation neutron energies. It would be of particular interest to expand the database to include SSF data derived using interrogation neutron spectra tallied in different matrix materials. The software algorithms established in this work provide a framework that can be arbitrarily expanded to include any data set. Consequently, although the focus of this work has been on DDA measurements, there is no software limitation in including self-shielding data sets derived for other active neutron interrogation assay system, such as Cf-shuffler. To make the software more accessible, future work may also cater for a graphical user interface to be developed.

REFERENCES

- [1] R.D. McElroy, Jr., S. Croft, B. Young, and L. C-A Bourva; “*Design and Performance of the Integrated Waste Assay System (IWAS)*”; Proceedings of the Institute of Nuclear Materials Management, 44th Annual Meeting, Phoenix (2003).
- [2] C. Passard, A. Mariani, F. Jallu, J. Romeyer-Dherber, H. Recroix, M. Rodriguez, J. Lorida, C. Denis, “*PROMETHEE: an alpha low level waste assay system using passive and active neutron measurement methods.*”; Nucl. Technol. 140, Dec 2002, 303–314.
- [3] E. Alvarez, C. Wilkins, S. Croft, M. Villani, A. Ambrifi, G. Simone; “*PANWAS: A Passive/Active Neutron Waste Assay System for the Radiological Characterization of Waste Packages at the Nucleco Facility at Casaccia*”; 2006 Waste Management Symposium, 26th Feb. – 2nd March 2006, Tucson, Arizona, USA.
- [4] L. C-A Bourva, S. Croft, P.M.J. Chard; “*The Effect of Self-Shielding in Active Neutron Assay of Plutonium Bearing Aggregates*”; Proceedings of the 8th NDA Waste Characterization Conference, Denver, Colorado, 11th-12th Dec. 2001, 116-122.
- [5] P.M.J. Chard and S. Croft; “*Self-Shielding Factor for the Cf Shuffler Neutron Interrogation Technique*”; Proceedings of the 17th Annual ESARDA Symposium on Safeguard and Nuclear Material Management, EUR 16290 EN, Aachen, Germany, 9th-11th May 1995, 557-562.
- [6] Denise B. Pelowitz, editor; “*MCNPX– User’s Manual, Version 2.7.0*”; LA-CP-11-00438 (April 2011).